

Fig. 2. INTI's AC-QVM. A: Clock generator. B: Signal generators. C: DUT. D:  $\Sigma\Delta$  digitizer. E: Programmable current source. F: Microwave generator. G: Liquid Helium dewar where the Josephson array is cooled down to 4.2 K. A and F are locked to INTI's Cesium atomic clock frequency.

### III. MEASUREMENT TECHNIQUES

The AC-QVM measures the difference between the DUT output signal and the reference signal synthesized by the PJVS as stated in section II. Then, the DUT signal is obtained by summing the sampled data plus the reference signal, this process is depicted in Fig. 3. As can be seen in Fig. 3-(b), the resulting signal has transients, due to the response of the  $\Sigma\Delta$  digitizer's digital 48-tap FIR filters to the transition between adjacent quantum voltage levels of the PJVS, these filters need a certain amount of samples to settle (24 in this application), where a highest accuracy level is of utmost importance condition to reach a better uncertainty level. Such transients can mislead the final result, therefore they must be removed from the resulting signal. To accomplish this, two methods were developed and compared. For which sine waveforms of 1 V amplitude with frequencies of 62.5 Hz and 31.25 Hz which are close to the industrial electrical power frequency range, were measured using the AC-QVM. The signals generated by the PJVS were synthesized with 20 steps per period, having the same amplitude and frequency as the generator (DUT) output signal, in such a way that the difference is close to tens of mV and digitized to an equivalent sampling rate of 32.5 kHz.

The following subsections describe the reconstruction of the signal and the two methods developed.

#### A. Method 1

The goal of these methods is to reconstruct the DUT signal while eliminating the transients and filling the time gap, in order to have a full signal according to the sampling rate and signal frequency ratio. This task is carried out in a two-step process: first, in-phase signals are sampled (signal 1 in Fig. 4-(a)); second, the unknown signal is set out-of-phase to the reference and sampled again (signal 2 in Fig. 4-(a)). This process results in two differential signals as illustrated in

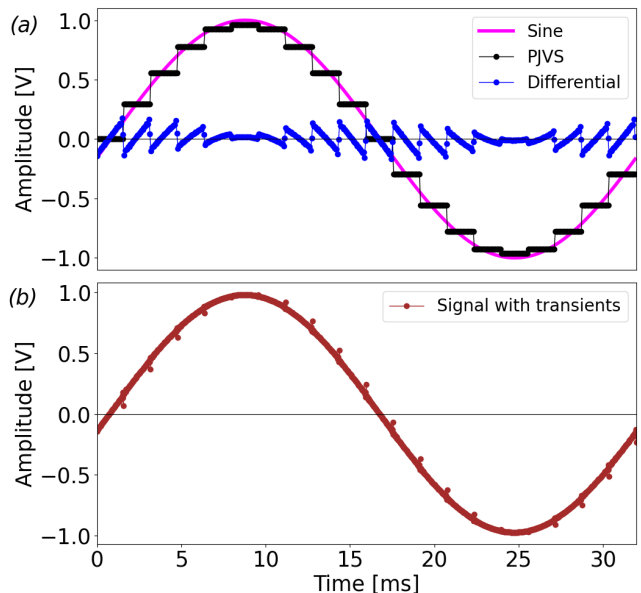


Fig. 3. Comparison of the signals. (a) The pink curve represents the ideal sine wave, while the black curve shows the ideal programmed PJVS signal. The blue curve depicts the measured differential signal. In (b), the reconstructed waveform with transients is displayed. Both methods described in the text are designed to eliminate these transients.

Fig. 4-(a). Then, to each differential signal, the PJVS reference values are added, as shown in Fig. 5-(a) where the phase shift ( $\Delta\phi$ ) between the signals can be seen. After this stage, the transients are removed. The final step consists of the combination of both signals resulting in a final signal without any time gap, as depicted in Fig. 5-(b).

The flow diagram of Fig. 6 describes the steps carried out for the signal reconstruction, where the PJVS block corresponds to the signal generated in the PJVS being the same for both measurements.

The TE blocks perform the transients elimination process, the input signal is separated into steps and then, the transients are removed. The difference between these blocks is that one of them eliminates the counterpart of points in the other. For example, if a step of a signal has 60 points and 20 points have to be eliminated, the TE block of signal 1 eliminates 10 points from the beginning and 10 from the end of the step, resulting in 40 remaining points for each step. The TE block of signal 2 will do the opposite, eliminating 40 points of the 60, 20 from each side of the step, and 20 points will be obtained for each step of the signal. At the end of this process, two signals with gaps due to the transient elimination are obtained. The RECO block combines both signals, filling the gaps of each step from both signals.

#### B. Method 2

In this method, the transients elimination and signal reconstruction procedure is the same as in *Method 1*, but the inputs are different. Instead of shifting the phase of the unknown signal, a second Josephson signal is generated,

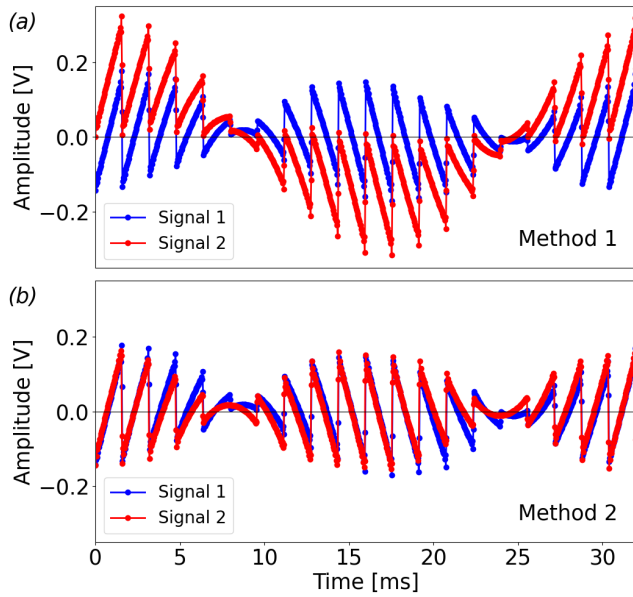


Fig. 4. Comparison of differential signals. Upper panel (a) shows the signals used in *Method 1*, a phase-shift is applied to signal 1 (blue) resulting in signal 2 (red). The lower panel (b) presents the differential signals used in *Method 2*, signal 2 (red) results from a new Josephson signal having the same number of steps but phase-shifted from the one used in signal 1 (blue), as described in the text.

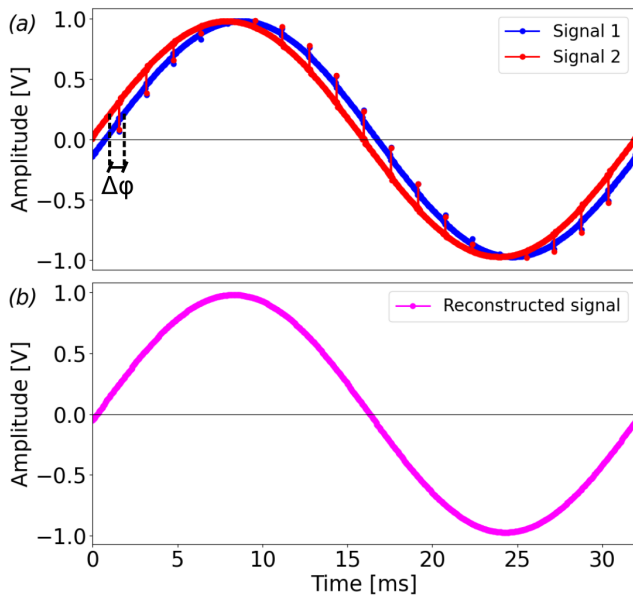


Fig. 5. This figure presents the signals used in *Method 1*. In (a) is shown the comparison between the two reconstructed signals presented in Fig. 4-(a), notice that both signals present transients. After applying the proposed method the waveform presented in (b) is obtained.

having the same number of steps as the initial signal in such a way that the position of the steps matches the necessary phase to occupy the transients positions. Then, a zero-crossing differential sampling is performed with respect to the generator

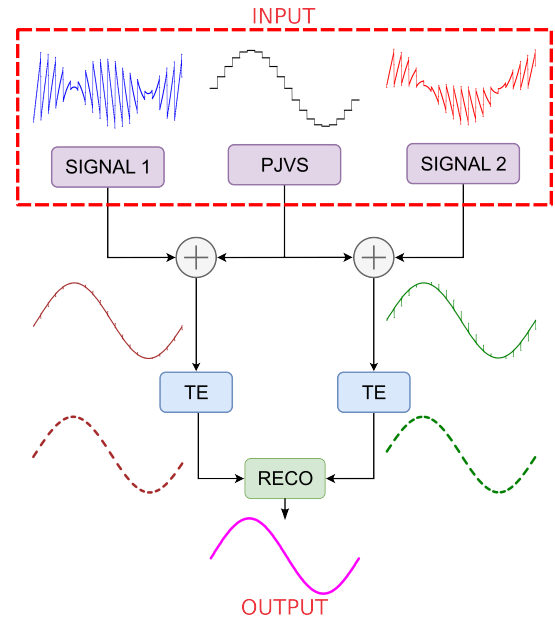


Fig. 6. Flow diagram of *Method 1*. The TE blocks correspond to the transients elimination process and RECO to the recombination of the signal.

signal. The Flow diagram of this technique is shown in Fig. 7.

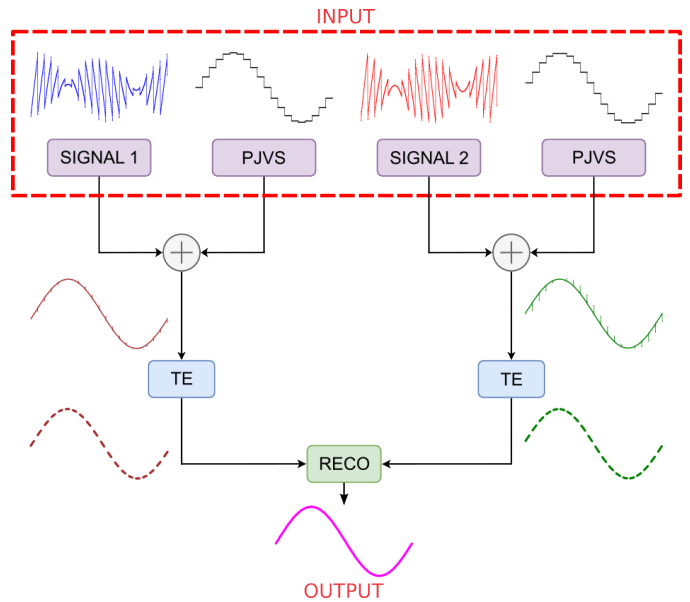


Fig. 7. Flow diagram of *Method 2*. The TE blocks correspond to the transients elimination process and RECO to the recombination of the signal, which are the same as *Method 1*.

#### IV. RESULTS

Having reconstructed the signal with both methods, the Root Mean Square (RMS) value was calculated and a stability analysis was carried out using Allan deviation [6]. The latter determines the minimum uncertainty that can be obtained in a given observation time or, as in this case, the number of signal periods that are necessary to perform subsequent calculations.

The time determined by the Allan deviation was 2.5 s. This translates into 156 periods for the 62.5 Hz frequency signal and 78 periods for the 31.25 Hz.

An example of the procedure carried out for a 31.25 Hz signal is shown in Fig. 8. The total input data has 500 periods, and taking as reference the Allan deviation time it was divided into 6 groups of 78 periods. Then, each group was divided again into 15 subgroups in a set of 5 periods to eliminate the 50 Hz interference on the measurements. On each set of 5 periods, the RMS value was performed. Then, over the resulting values, the average is calculated resulting in six independent  $RMS_k$ ,  $k = 1, \dots, 6$  values, and its corresponding standard deviation was performed. Finally, the total RMS value  $RMS_T$  was obtained by averaging the previous results ( $RMS_k$ ), and the type-A uncertainty was calculated. This uncertainty value was obtained from the standard deviation of each group. All the calculations were performed with integer divisions, discarding the surplus.

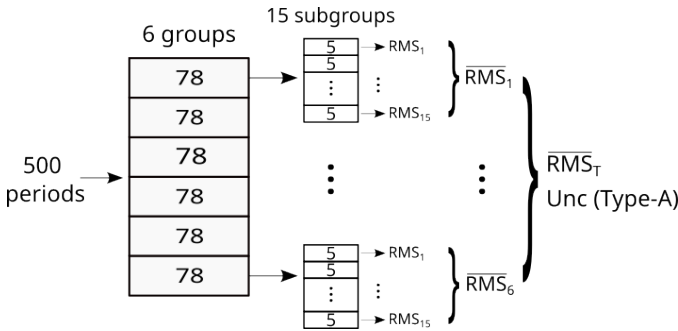


Fig. 8. Diagram of the procedure to calculate the results for a 31.25 Hz signal. The first set of 6 groups was divided taking into account the Allan deviation time and the second set of 15 subgroups correspond to the number of periods necessary to eliminate the 50 Hz interference. The final result is the total RMS value ( $RMS_T$ ) and the type-A uncertainty.

The transients elimination process required removing 28 points for the 31.25 Hz signal, and only 12 for the 62.5 Hz signal.

TABLE I

THIS TABLE SHOWS THE RMS VALUES CALCULATION RESULTS. NOMINAL ERROR IS THE DIFFERENCE OF EACH METHOD TO THE REFERENCE VALUE OF A SINE WAVEFORM. METHOD ERROR CORRESPONDS TO THE DIFFERENCE BETWEEN METHODS.

Frequency	Parameters	Method 1	Method 2
31.25 Hz	RMS value [V]	0.6916345	0.6919580
	Standard deviation [ $\mu$ V]	1.6	1.2
	Uncertainty [ $\mu$ V]	0.9	0.9
	Nominal error [mV]	15.472	15.149
	Method error [ $\mu$ V]	323.6	
62.5 Hz	RMS value [V]	0.6916783	0.6919972
	Standard deviation [ $\mu$ V]	0.6	1.7
	Uncertainty [ $\mu$ V]	0.9	1.0
	Nominal error [mV]	15.428	15.120
	Method error [ $\mu$ V]	318.9	

Table I shows the results obtained from the analysis made, where it can be seen that both methods have similar results. The differences to the nominal peak amplitude of 1 V are

about 15 mV, and the agreement between methods is about 300  $\mu$ V. The type-A uncertainty of both methods was close to 0.9  $\mu$ V.

Furthermore, *Method 1* requires a manual adjustment for determining the phase of the signal required for the measurements, leading to an increased execution time. Instead, *Method 2* requires less execution time as the generation of the PJVS is only modified once before the measurement is performed.

## V. CONCLUSION

A comparison between the two methods for differential measurements was presented. Each of the methods was described and an analysis of the RMS value of 31.25 Hz and 62.5 Hz signals was performed. The results indicated that the differences concerning a nominal value of 1 V amplitude were about 15 mV, and the difference between both methods was close to 300  $\mu$ V. Also, the type-A uncertainty of both was about 0.9  $\mu$ V.

It is concluded that *Method 2* outperforms *Method 1* in terms of accuracy and efficiency.

Moreover, *Method 1* requires a longer execution time of measurement, allowing extra possible errors. In contrast, *Method 2* only requires a single modification of the PJVS generation before performing the measurement.

Furthermore, these methods offer an advantage over conventional techniques as they enable a more comprehensive time and frequency analysis since the resulting signal contains more information and the gaps of the transients are eliminated.

## ACKNOWLEDGMENT

The authors thank Dr. Ralf Behr and Dr. Luis Palafox of the PTB for their constant support in the setup process of the Josephson system.

## REFERENCES

- [1] B. D. Josephson, "Possible new effects in superconductive tunnelling," *Physics letters*, vol. 1, no. 7, pp. 251–253, 1962.
- [2] J. Kohlmann and R. Behr, *Development of Josephson voltage standards*. Wiley-VCH, 07 2011.
- [3] B. Jeanneret and S. Benz, "Application of the josephson effect in electrical metrology," *The European Physical Journal Special Topics*, vol. 172, pp. 181–206, 06 2009.
- [4] R. J. Iuzzolino, "Josephson waveforms characterization of a sigma-delta analog-to-digital converter for data acquisition in metrology," Ph.D. dissertation, B-IGSM, Berlin, Aug 2011. [Online]. Available: [https://publikationsserver.tu-braunschweig.de/receive/dbbs\\_mods\\_00042711](https://publikationsserver.tu-braunschweig.de/receive/dbbs_mods_00042711)
- [5] R. Iuzzolino, M. E. Bierzychudek, L. Palafox, R. Behr, and A. Tedesco, "On the development of an ac-quantum voltmeter," in *2018 Conference on Precision Electromagnetic Measurements (CPEM 2018)*, 2018, pp. 1–2.
- [6] T. Witt, "Using the allan variance and power spectral density to characterize dc nanovoltmeters," *Instrumentation and Measurement, IEEE Transactions on*, vol. 50, pp. 445 – 448, 05 2001.